Chinese Chemical Letters 32 (2021) 2509–2512

Contents lists available at ScienceDirect

Chinese Chemical Letters

journal homepage: www.elsevier.com/locate/cclet

Communication

Activity enhancement of acetate precursor prepared on MnO_x-CeO_2 catalyst for low-temperature NH_3-SCR: Effect of gaseous acetone addition

Lyumeng Ye[a,b], Peng Lu[b,c], Dingsheng Chen[b,c], Dongyao Chen[b,c], Haiwen Wu[b,c], Wenjing Dai[a], Yanling Gan[a], Jiayong Xiao[d], Zongwei Xie[e], Zengwang Li[d], Haibao Huang[a,*]

[a] School of Environmental Science and Engineering, Sun Yat-sen University, Guangzhou 510275, China
[b] The Key Laboratory of Water and Air Pollution Control of Guangdong Province, South China Institute of Environmental Sciences, The Ministry of Ecology and Environment of PRC, Guangzhou 510655, China
[c] Guangdong Province Engineering Laboratory for Air Pollution Control, South China Institute of Environmental Sciences, The Ministry of Ecology and Environment of PRC, Guangzhou 510655, China
[d] Zhuhai Jinwan Liangang Foundation Investment Co., Ltd., Zhuhai 519090, China
[e] Hunan Construction Engineering Group, Changsha 410000, China

ARTICLE INFO

Article history:
Received 17 October 2020
Received in revised form 24 November 2020
Accepted 23 December 2020
Available online 25 December 2020

Keywords:
MnO_x-CeO_2 catalyst
Hydrolysis driving redox method
Low temperature NH_3-SCR
Acetate precursor
Effect of gaseous acetone

ABSTRACT

MnO_x-CeO_2 catalysts are developed by hydrolysis driving redox method using acetate precursor (3Mn1Ce-Ac) and nitrate precursor (3Mn1Ce-N) for the selective catalytic reduction (SCR) of NO_x by NH_3. A counterpart sample (Cop-3Mn1Ce) was prepared by the NH_3·H_2O co-precipitation method for comparison purpose. Combining the results of physicochemical properties characterization and performance test, we find that the 3Mn1Ce-Ac catalyst with some nanorod structures is highly active for the deNO_x process. The SCR activity of the 3Mn1Ce-Ac catalyst is more admirable than the 3Mn1Ce-N and the Cop-3Mn1Ce catalysts due to plentiful Lewis acid sites, excellent low-temperature reducibility, and superior surface area resulted from O_2 generation during the preparation procedure. The 3Mn1Ce-Ac still exhibits the greatest performance for the deNO_x process when gaseous acetone is in the SCR feed gas. The NO_x conversion and N_2 selectivity over the 3Mn1Ce-Ac are both improved by gaseous acetone above 150 °C due to the inhibition of SCR undesired side reactions (NSCR & C-O reactions) and "slow-SCR" process.

Selective catalytic reduction (SCR) with ammonia is an efficient way to control NO_x emission. Manganese oxide-based catalysts are gaining much attention due to the fact that they exhibit excellent low-temperature activity than V_2O_5-WO_3(MoO_3)/TiO_2 catalysts at the actual flue gas temperature (< 200 °C) [1–3]. However, one of the largest drawbacks of the pure MnO_x is its relatively narrow temperature range, which limits its practical use in the NH_3-SCR process [4]. Ce could be introduced into MnO_x, and Mn-Ce oxide possesses as a superior catalyst owes a good deal to the synergistic effects between MnO_x and CeO_2 [1,2,5].

Recent years, a novel hydrolysis driving redox method has been successfully applied to synthesize higher low-temperature activity Mn-Ce catalysts [6,7]. In this process, $KMnO_4$ reacts with metal ionic salts (*i.e.*, Ce^{3+}) in the presence of H_2O_2 solution (*i.e.*, $6MnO_4^-$ (aq) + $2Ce^{3+}$ (aq) + $9H_2O_2$ (l) = $6MnO_2$ (s) + $2Ce(OH)_3$ (s) + $6H_2O$ (l) + $9O_2$ (g)). And a MnO_x-CeO_2 catalyst with a stoichiometric ratio of Mn/Ce = 3 is subsequently synthesized. A large average pore size and a high S_{BET} which are beneficial to the catalytic performance are obtained due to a large amount of O_2 emitted during the procedure. The as-prepared 3Mn1Ce catalysts were reported to display strong reducibility and favorable performances in the removal of BTEX and chlorobenzene [6,7]. However, these superior MnO_x-CeO_2 catalysts have not been tested in the NH_3-SCR deNO_x process. Moreover, it should be noted that cerium(III) nitrate hexahydrate ($Ce(NO_3)_3$·$6H_2O$) employed in the preparation process was corrosive and very toxic to aquatic life with long-lasting effects. Meanwhile, some researches showed that catalysts prepared by nitrate (N) precursor exhibited lower activity than those prepared by acetate (Ac) precursor [8,9]. Thus, the present study chooses Ac precursor to prepare 3Mn1Ce catalysts by hydrolysis driving redox method. Also, the N precursor is applied for comparison purpose.

* Corresponding author.
E-mail address: seabao8@gmail.com (H. Huang).

https://doi.org/10.1016/j.cclet.2020.12.040

As one of the representatives of oxygenated VOCs (OVOCs), gaseous acetone usually coexists with NO_x in the flue gases from the incomplete combustion of fossil fuels, biomass, and solid wastes, *etc.* [10–13]. However, in contrast to many works focus on the effect of Cl-contained VOCs (Cl-VOCs, *e.g.*, chlorobenzene) and benzene series (*e.g.*, toluene) on the NH_3-SCR process, few researchers play attention to the impact of OVOCs (*e.g.*, acetone) [14,15]. Previous studies have been confirmed that chlorobenzene could improve the N_2 selectivity and widen the active temperature of SCR reaction, while toluene significantly inhibits the deNO_x activity and results in even poorer N_2 selectivity. Thus, it suggested that different VOCs will make different impacts on the NH_3-SCR reaction, and how gaseous acetone influence the NH_3-SCR process needs attention. To date, to the best of the authors' knowledge, there is only a very limited report studying the effect of gaseous acetone on the NH_3-SCR process.

In this work, 3Mn1Ce catalysts were synthesized using two methods: hydrolysis driving redox method (3Mn1Ce-Ac, and 3Mn1Ce-N) and $NH_3{\cdot}H_2O$ co-precipitation method (Cop-3Mn1Ce). In brief, $Ce(CH_3COO)_3{\cdot}xH_2O$ was the precursor for the 3Mn1Ce-Ac synthesis, while $Ce(NO_3)_3{\cdot}6H_2O$ for the 3Mn1Ce-N. N_2 adsorption-desorption isotherms, X-ray powder diffraction (XRD), scanning electron microscopy (SEM), transmission electron microscopy (TEM), H_2 temperature-programmed reduction (H_2-TPR), and NH_3 temperature-programmed desorption (NH_3-TPD), were applied to characterize the physicochemical properties of different catalysts. The activity of the catalyst was then tested by on-line FTIR (GASMET DX-4000). The possible impacts of gaseous acetone on SCR performance and SCR side reactions were finally investigated. Detail catalysts synthesis, experimental setup, and definition of the SCR side reactions were presented in Supporting information.

Fig. 1 shows the SCR performance of three 3Mn1Ce catalysts in the low temperature range of 50–200 °C. The light-off curves for NO_x conversion are typical convex curves due to the competition between NO reduction and NH_3 oxidation when the temperature increases. The 3Mn1Ce catalysts synthesized by hydrolysis driving redox method (3Mn1Ce-Ac and 3Mn1Ce-N) are more active than that synthesized by $NH_3{\cdot}H_2O$ co-precipitation method (Cop-3Mn1Ce). The temperatures T_{50} and T_{90} corresponding to NO_x conversions of 50% and 90%, respectively, are summarized to better show the catalytic activities. The T_{50} and T_{90} of 3Mn1Ce-Ac (66 and 105 °C) were lower than that of 3Mn1Ce-N (74 and 117 °C), It is obvious that the acetate precursor was superior for the preparation of higher low-temperature activity MnO_x-CeO_2 catalysts in hydrolysis driving redox method.

To better explain the catalytic performance of the prepared catalysts, detailed physicochemical characterizations are carried out. The XRD results of the 3Mn1Ce catalysts are depicted in Fig. S1 (Supporting information). It could be seen that all the diffraction peaks are broad, indicating the low crystallinity of the 3Mn1Ce catalysts. Some small peaks corresponding to MnO_2 (JCPDS PDF# 72–1982) are found in the 3Mn1Ce-Ac catalyst. According to the high-resolution transmission electron microscopy (HRTEM) images of the 3Mn1Ce-Ac catalyst, some nanorod structures are presented (Fig. 2a). These structures are not observed in 3Mn1Ce-N and Cop-3Mn1Ce catalysts (Fig. S2 in Supporting information). The element distribution mappings of Mn and Ce demonstrate that the MnO_2 nanorods are formed, and Ce cations are introduced into the nanorods structure (Figs. 2b and c) [16]. Besides, some lattice defects can be identified in the image (Fig. 2d). The introduction of Ce ions into the lattice matrix of MnO_2 nanorods is favorable for the occurrence of lattice defects [7], which promotes the formation of more oxygen vacancies and subsequently enhances the catalytic performance of the 3Mn1Ce-Ac.

The as-prepared 3Mn1Ce catalysts are mesoporous structures according to the N_2 isotherms [17] (Fig. S3a in Supporting information). However, the pore size distributions of these catalysts are different (Fig. S3b in Supporting information). Compared with the Cop-3Mn1Ce catalyst, two 3Mn1Ce catalysts synthesized by hydrolysis driving redox method are abundant in mesopores (2–50 nm) due to the inhibition of small particles agglomeration by the O_2 produced during the preparation procedure [7,18]. Moreover, the pore size of the 3Mn1Ce-Ac catalyst is mainly distributed in the range of 7–30 nm, while the majority of the pore size of the 3Mn1Ce-N catalyst is less than 5 nm. Surface morphologies by SEM well confirm the above phenomena (Figs. S4a, S4b and S4d in Supporting information). The BET surface area of the catalyst decreases in the order: 3Mn1Ce-Ac > Cop-3Mn1Ce > 3Mn1Ce-N (Table S1 in Supporting information). 3Mn1Ce-Ac catalyst has the largest BET surface area (145.36 m^2/g), pore volume (0.82 cm^3/g), and pore diameter (23.87 nm), which are beneficial for the contact of reactants and the occurrence of reactions due to more available active sites provided on the catalyst surface.

Redox properties and surface acidity of the catalyst play important roles in the NO_x reduction. Redox properties determined by H_2-TPR are displayed in Fig. S5a and Table S2 (Supporting information). Two obvious reduction peaks in the range of

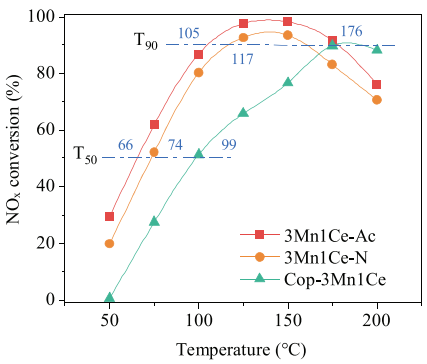

Fig. 1. NO_x conversion over 3Mn1Ce catalysts. Reaction conditions: $[NH_3]$ = [NO] = 500 ppm, O_2 = 10 vol%, GHSV = 60,000 mL g^{-1} h^{-1}.

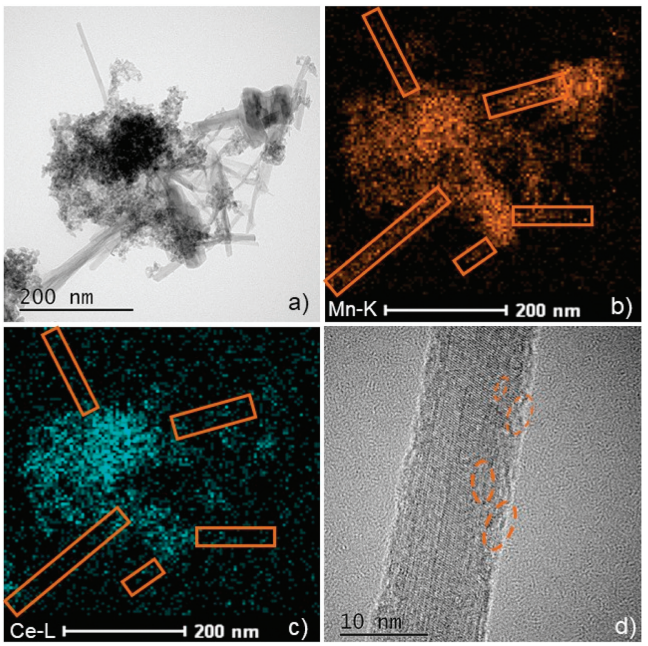

Fig. 2. Studies of the 3Mn1Ce-Ac catalyst by TEM (a) TEM image, (b) Mn-element mapping, (c) Ce-element mapping, (d) HRTEM image of the nanorod.

200−400 °C are observed over three 3Mn1Ce catalysts as reported in previous studies [7,19], associating with two stepwise reductions of Mn^{4+} to Mn^{3+} and Mn^{3+} to Mn^{2+}, overlapping the reduction of surface Ce^{4+}. Compared with the reduction peaks of CeO_2 (> 450 °C) and MnO_x (~400 °C) (Fig. S6 in Supporting information), the values of 3Mn1Ce catalysts are significantly lower. This result is related to the formation of a solid solution with Mn-O-Ce structures, which improves the mobility of oxygen species (O_2^-, O_2^{2-} and O^-) greatly and makes catalysts surface more reducible [20,21]. The reduction peak of the 3Mn1Ce-Ac starts at 89 °C, which is lower than that of 3Mn1Ce-N (118 °C) and Cop-3Mn1Ce (97 °C). This result indicates that oxygen vacancy can be formed at such a low temperature, which provides the possibility for a low-temperature operation to remove NO_x. To further investigate the reducibility of three 3Mn1Ce catalysts, the amount of H_2 consumption with AgO as standard material is calculated. H_2-TPR curves are fitted by Gaussian function with a fitting quality R^2 higher than 0.99. The total H_2 consumption is ranked in the order: 3Mn1Ce-Ac > 3Mn1Ce-N > Cop-3Mn1Ce. The H_2 consumption of the 3Mn1Ce-Ac catalyst reaches 7.85 mmol/g, suggesting that a large amount of most active oxygen is involved in the reaction [20,22]. Moreover, the H_2 consumption rate (Fig. S5b, detailed calculation see Supporting information) of 3Mn1Ce-Ac is the highest with the largest temperature range among three catalysts, inferring that the 3Mn1Ce-Ac catalyst poses outstanding oxygen migration ability within a wider temperature range, which is consistent with the deNO_x performance.

NH_3-TPD is applied to quantify the surface acid amount of 3Mn1Ce catalysts, and the results are presented in Fig. S7 (Supporting information) and Table S2. It is obvious that 3Mn1Ce catalysts synthesized by different methods all present multi-desorption peaks. As previous literature reported, physisorbed NH_3 desorption associated with weak acid sites always happens below 400 °C and probably relates to Brønsted acid sites, while chemisorbed NH_3 desorption associated with strong acid sites would occur above 400 °C and assigns to Lewis acid sites [23–26]. Since the area of desorption peaks can clearly show the surface acid amount, quantitative analysis by integrating the NH_3-TPD curves is performed. 3Mn1Ce-Ac catalyst has the largest surface acid amount (1.76 mmol/g) for NH_3 adsorption among the three 3Mn1Ce catalysts. In the meantime, the contribution of strong acid sites follows the order of 3Mn1Ce-Ac > 3Mn1Ce-N > Cop-3Mn1Ce, which is consistent with the catalytic performance in NH_3-SCR reaction, indicating that the strong acid sites assigned to Lewis acid are highly correlated with catalytic activity.

3Mn1Ce-Ac catalyst still exhibits an excellent SCR activity when gaseous acetone is in the feed gas (Fig. S8 in Supporting information). The impact of gaseous acetone on NO_x conversion and N_2 selectivity are then evaluated over the 3Mn1Ce-Ac catalyst (Fig. 3). When the temperature is below 150 °C, the NO_x conversion and N_2 selectivity decrease when acetone is introduced into the flue gas. However, when the temperature is higher than 150 °C, these two indicators are improved.

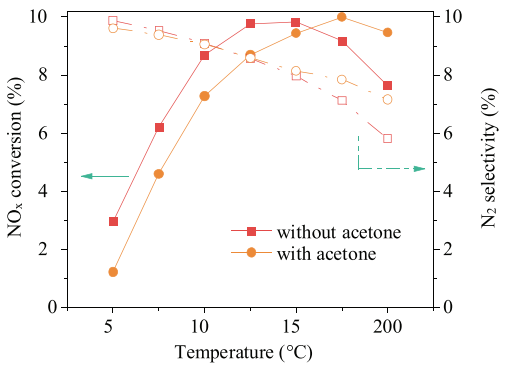

Fig. 3. The impact of gaseous acetone on NO_x conversion and N_2 selectivity over the 3Mn1Ce-Ac catalyst. Reaction conditions: [NH_3] = [NO] = 500 ppm, [acetone] = 50 ppm (when used), O_2 = 10 vol%, GHSV = 60,000 mL g^{-1} h^{-1}.

Fig. 4a shows the byproduct N_2O concentration in the SCR reaction without/with gaseous acetone. It is obvious that N_2O concentration decreases when gaseous acetone is added. The NSCR reaction ($4NH_3 + 4NO + 3O_2 \rightarrow 4N_2O + 6H_2O$) is suppressed by gaseous acetone. As a consequence, more NH_3 can participate in the standard SCR reaction when gaseous acetone is present, resulting in a positive effect on the N_2 selectivity. At the same time, gaseous acetone restrains the NH_3 catalytic oxidation reaction (C-O reaction: $4NH_3 + 5O_2 \rightarrow 4NO + 6H_2O$ and $2NH_3 + 2O_2 \rightarrow N_2O + 3H_2O$). The concentration of NH_3 oxidation by-products (N_2O + NO) significantly decrease, resulting in more available NH_3 in the SCR reaction (Fig. 4b). The conjunction of these results reveals that gaseous acetone inhibits the SCR side reactions over the 3Mn1Ce-Ac catalyst.

On the other hand, the NO_2 fraction affects the reaction paths of NH_3-SCR [27]. As is generally accepted, the deNO_x activity will be improved through the so-called 'fast-SCR' process with NO_2 concentration increasing. However, when NO_2/NO_x > 50%, NO reduction is mainly controlled by 'slow-SCR' reaction (NO_2-SCR reaction), and higher NO_2 concentration will limit the deNO_x activity. As illustrated in Fig. 4c, a condition of NO_2/NO_x < 50% is identified at 100 ℃, suggesting that the so-called 'fast-SCR' process determines the NH_3-SCR reaction. On the contrary, the percentage of NO_2/NO_x increases to more than 50% at 200 ℃, and the NH_3-SCR process shifts to 'slow-SCR'. In addition, gaseous acetone inhibits the NO_2 formation as shown in Fig. 4d. Thus, it is clear that lower NO_2 concentration in the NH_3-SCR reaction with acetone at 100 ℃ reduces the percentage of the 'fast-SCR' process, leading to a decrease of SCR activity. In contrast, slow SCR reaction is limited by lower NO_2 concentration at 200 ℃, thus, results in the enhancement of deNO_x activity.

For the purpose of comparison, the impacts of gaseous acetone on SCR performance and SCR side reactions over the 3Mn1Ce-N catalyst are also investigated (Fig. S9 in Supporting information). The tendency of NO_x conversion is in consistent with the 3Mn1Ce-

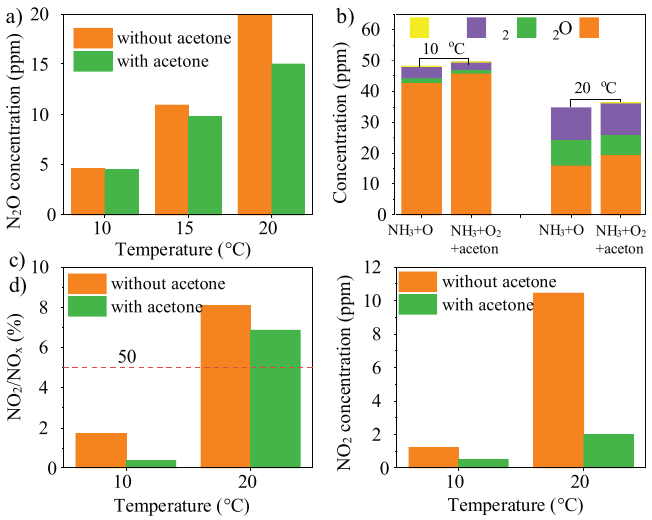

Fig. 4. (a, c, d) N_2O concentration, NO_2/NO_x percentage and NO_2 concentration in the NH_3-SCR reaction without/with acetone, and (b) the effect of acetone on the NH_3 catalytic oxidation over the 3Mn1Ce-Ac catalyst. Reaction conditions: [NH_3] = [NO] = 500 ppm (when used), [acetone] = 50 ppm (when used), O_2 = 10 vol%, GHSV = 60,000 mL g^{-1} h^{-1}.

Ac catalyst. However, the N_2 selectivity exhibits an opposite trend over the 3Mn1Ce-N catalyst compared with the 3Mn1Ce-Ac catalyst. Gaseous acetone facilitates the NSCR process to produce more N_2O, leading to a decrease of N_2 selectivity (Fig. S10 in Supporting information).

Overall, three different 3Mn1Ce catalysts synthesized by hydrolysis driving redox method (3Mn1Ce-Ac, and 3Mn1Ce-N) and $NH_3{\cdot}H_2O$ co-precipitation method (Cop-3Mn1Ce) are used for NH_3-SCR. Among them, the 3Mn1Ce-Ac catalyst with some nanorod structures prepared by acetate (Ac) precursor exhibits the greatest SCR performance. Such a favorable deNO_x behavior of 3Mn1Ce-Ac catalyst is mainly attributed to its large surface area for more available active sites, plentiful Lewis acid sites, and excellent low-temperature reducibility. Gaseous acetone inhibits the SCR undesired side reactions (NSCR & C-O reactions) and limits the "slow-SCR" process over 3Mn1Ce-Ac catalyst above 150 °C, resulting in the enhancement of NO_x conversion and N_2 selectivity. Different from the 3Mn1Ce-Ac catalyst, the 3Mn1Ce-N catalyst displays weak capacity against NSCR reaction, leading to poor N_2 selectivity.

Declaration of competing interest

The authors report no declarations of competing interest.

Acknowledgments

This work was supported by the Key Laboratory of Water and Air Pollution Control of Guangdong province, China (No. 2017A030314001), the National Key Research and Development Plan (No. 2019YFC0214303), Central Public-Interest Scientific Institution Basal Research Fund (No. PM-zx703-202002-015), and the National Natural Science Foundation of China (No. 22076224).

Appendix A. Supplementary data

Supplementary material related to this article can be found, in the online version, at doi:https://doi.org/10.1016/j.cclet.2020.12.040.

References

[1] L.P. Han, S.X. Cai, M. Gao, et al., Chem. Rev. 119 (2019) 10916–10976.
[2] C. Liu, J.W. Shi, C. Gao, et al., Appl. Catal. A 522 (2016) 54–69.
[3] C. He, J. Cheng, X. Zhang, et al., Chem. Rev. 119 (2019) 4471–4568.
[4] Y. Geng, W.P. Shan, F.D. Liu, et al., J. Hazard. Mater. (2020) 124223-124223.
[5] G.S. Qi, R.T. Yang, Chem. Commun. (2003) 848–849.
[6] J. Chen, X. Chen, W.J. Xu, et al., Chem. Eng. J. 330 (2017) 281–293.
[7] J. Chen, X. Chen, X. Chen, et al., Appl. Catal. B 224 (2018) 825–835.
[8] J.H. Li, J.J. Chen, K. Rui, et al., Catal. Commun. 8 (2007) 1896–1900.
[9] F. Kapteijn, L. Singoredjo, M. Vandriel, et al., J. Catal. 150 (1994) 105–116.
[10] H. Huang, H. Hu, J.J. Zhang, et al., Environ. Res. 188 (2020) 109802.
[11] J.M. Chen, C.L. Li, Z. Ristovski, et al., Sci. Total Environ. 579 (2017) 1000–1034.
[12] M.L. Wang, S.Y. Li, R.C. Zhu, et al., Atmos. Environ. 223 (2020) 117294.
[13] Q. Zhao, Q.L. Liu, J.F. Han, et al., J. Chem. Technol. Biotechnol. 94 (2019) 3753–3762.
[14] L.M. Ye, P. Lu, X.B. Chen, et al., Appl. Catal. B 277 (2020) 119257.
[15] L.N. Gan, K.Z. Li, S.C. Xiong, et al., Catal. Commun. 117 (2018) 1–4.
[16] J. Chen, X. Chen, D.X. Yan, et al., Appl. Catal. B 250 (2019) 396–407.
[17] Q. Shen, L.Y. Zhang, N.N. Sun, et al., Chem. Eng. J. 322 (2017) 46–55.
[18] J. Chen, X. Chen, Z. Xu, et al., ChemistrySelect 1 (2016) 4052–4056.
[19] X.J. Yao, K.L. Ma, W.X. Zou, et al., Chinese J. Catal. 38 (2017) 146–159.
[20] P.F. Zhang, H.F. Lu, Y. Zhou, et al., Nat. Commun. 6 (2015) 8446.
[21] W.L. Cen, Y. Liu, Z.B. Wu, et al., Phys. Chem. Chem. Phys. 14 (2012) 5769–5777.
[22] K. Qi, J.L. Xie, Z. Zhang, et al., Powder Technol. 338 (2018) 774–782.
[23] D.S. Zhang, L. Zhang, L.Y. Shi, et al., Nanoscale 5 (2013) 1127–1136.
[24] Z.B. Wu, R.B. Jin, Y. Liu, et al., Catal. Commun. 9 (2008) 2217–2220.
[25] R.B. Jin, Y. Liu, Z.B. Wu, et al., Chemosphere 78 (2010) 1160–1166.
[26] L. Chmielarz, P. Kuśtrowski, M. Zbroja, et al., Appl. Catal. B 53 (2004) 47–61.
[27] M. Iwasaki, H. Shinjoh, Appl. Catal. A. 390 (2010) 71–77.